

PAPER

Exploring the role of genome and structural ions in preventing viral capsid collapse during dehydration

To cite this article: Natalia Martín-González *et al* 2018 *J. Phys.: Condens. Matter* **30** 104001

View the [article online](#) for updates and enhancements.

Related content

- [Structural transitions in Cowpea chlorotic mottle virus \(CCMV\)](#)
Lars O Liepold, Jennifer Revis, Mark Allen et al.
- [Assembly/disassembly of a complex icosahedral virus to incorporate heterologous nucleic acids](#)
Elena Pascual, Carlos P Mata, José L Carrascosa et al.
- [Length of encapsidated cargo impacts stability and structure of in vitro assembled alphavirus core-like particles](#)
Vamseedhar Rayaprolu, Alan Moore, Joseph Che-Yen Wang et al.

Recent citations

- [Special Issue on the Physics of Viral Capsids](#)
Marek Cieplak and Wouter H Roos



IOP | ebooks™

Bringing you innovative digital publishing with leading voices to create your essential collection of books in STEM research.

Start exploring the collection - download the first chapter of every title for free.

Exploring the role of genome and structural ions in preventing viral capsid collapse during dehydration

Natalia Martín-González¹, Sofía M Guérin Darvas^{2,6}, Aritz Durana^{3,4}, Gerardo A Marti⁵, Diego M A Guérin^{2,3}  and Pedro J de Pablo¹ 

¹ Departamento de Física de la Materia Condensada C-III and Instituto de Física de la Materia Condensada (IFIMAC), Universidad Autónoma de Madrid, Cantoblanco 28049 Madrid, Spain

² Department of Biochemistry and Molecular Biology, University of the Basque Country (UPV/EHU), Barrio Sarriena S/N, 48940, Leioa, Vizcaya, Spain

³ Instituto Biofisika (IBF, UPV/EHU, CSIC), Parque Científico de la UPV/EHU, Barrio Sarriena S/N, 48940, Leioa, Vizcaya, Spain

⁴ Fundación Biofísica Bizkaia, Edificio Biblioteca Central UPV/EHU, Bº Sarriena S/N, 48940, Leioa, Vizcaya, Spain

⁵ Centro de Estudios Parasitológicos y de Vectores (CEPAVE-CCT-La Plata-CONICET-UNLP), Boulevard 120 e/61 y 62, 1900 La Plata, Argentina

E-mail: p.j.depablo@uam.es (P J de Pablo) and diego.guerin@ehu.eus (D M A Guérin)

Received 18 September 2017, revised 12 January 2018

Accepted for publication 19 January 2018


Published 15 February 2018



Abstract

Even though viruses evolve mainly in liquid milieu, their horizontal transmission routes often include episodes of dry environment. Along their life cycle, some insect viruses, such as viruses from the *Dicistroviridae* family, withstand dehydrated conditions with presently unknown consequences to their structural stability. Here, we use atomic force microscopy to monitor the structural changes of viral particles of *Triatoma virus* (TrV) after desiccation. Our results demonstrate that TrV capsids preserve their genome inside, conserving their height after exposure to dehydrating conditions, which is in stark contrast with other viruses that expel their genome when desiccated. Moreover, empty capsids (without genome) resulted in collapsed particles after desiccation. We also explored the role of structural ions in the dehydration process of the virions (capsid containing genome) by chelating the accessible cations from the external solvent milieu. We observed that ion suppression helps to keep the virus height upon desiccation. Our results show that under drying conditions, the genome of TrV prevents the capsid from collapsing during dehydration, while the structural ions are responsible for promoting solvent exchange through the virion wall.

Keywords: icosahedral non-enveloped viruses, hydrophobic gate, *Triatoma virus*, virus dehydration, AFM, atomic force microscopy

 Supplementary material for this article is available [online](#)

(Some figures may appear in colour only in the online journal)

⁶ Current address: Faculty of Biology and Phycology, Gottingen University, Wilhelm-Weber-Str. 2 D-37073 Göttingen. Germany.

Introduction

Viral modes of infection divide into two main routes: vertical transmission, which is from a host to its progeny, and horizontal transmission, which occurs through direct or indirect host-to-host contacts. The horizontal route can include a large variety of environmental agents like aerosol spread, and food or water up-taking. Since it is assumed that most viruses are highly sensitive to desiccation [1], the ability of the virus to stand ambient conditions is a limiting factor for virus spread. In this respect, aspects like resistance to dehydration and virus spread through contaminated fomites, are important factors that affect the transmission of several viral human diseases [1–6]. Nevertheless, the molecular determinants by which viral structures resist desiccation remain unknown.

Some prototypical human viruses are poliovirus (PV) [7], hepatitis A virus (HAV) [8], and human rhino virus (HRV) [9]. Their structures show some common features: they are spherical structures of about 30 nm in diameter, built of 60 copies of four different peptides, and lack of an outer lipid bilayer envelope. These protein shells are compact with no obvious holes through which the internal solvent could be exchanged with that of the surrounding external milieu. However, the capsid presents cavities that traverse along the five-fold icosahedral axes. These cavities are constructed by an annulus formed by the five symmetry-related amino acid side chains, and this constriction is of about 0.4 nm in diameter. In many virus structures, an electron density is observed at this point, and has been interpreted as coordinated divalent cations that seem to block the cavity [10–13]. These metal ions are accessible from the external solvent and can be removed by chelating agents [10, 14, 15]. Although the putative function of these ions most likely relates to capsid stability, their structural role has not been experimentally determined yet.

Within the order *Picornavirales*, *Dicistroviridae* is a family that groups 15 viral pathogens of several arthropods of economic importance. For example, the *Cricket paralysis virus* (CrPV) infects field crickets (*Teleogrillus oceanicus* and *T. commodus*), causing great losses in agriculture worldwide; and the *Black queen cell virus* (BQCV) and *Israeli acute paralysis virus* (IAPV) are two pathogens that represent major threats to honeybee (*Apis mellifera*) populations. However, among dicistroviruses, *Triatoma virus* (TrV) is the only reported virus that infects the hematophagous insects known as triatomines (*Hemiptera:Reduviidae*).

Empty TrV particles (devoid of genome) were observed in intestine samples of both alive and dead triatomines [16]. Together with these natural empty particles, two other empty particles can be obtained by experimental techniques [17]. These three empty particles were chemically characterized; their structures were solved at low resolution by transmission electron microscopy (TEM) reconstructions [18], and one of them at medium resolution by x-ray crystallography [19]. These studies allowed us to conclude that the three empty particles, and most likely the ones observed by direct TEM images taken from fresh feces, are almost identical to the atomic structure of full particles obtained by crystallography. Another conclusion was that the misprocessing of the

precursor of the capsid proteins can produce different peptides, but even so they are able to assemble into spherical particles of the same diameter (~30 nm). However, these are unable to incorporate the viral RNA [17].

Despite the hosts' diversity of dicistroviruses, one common characteristic in their life cycle is that the main route of transmission is *per os* [20]. This transmission mode implies that their viral capsids are strong enough to stand the harsh conditions they encounter through the digestive tract pathway of the insect. In the case of TrV, the virus may remain intact for years within infected dead insects [21], showing that the capsid resists the proteases and nucleases released by the decaying corpses. Additionally, both CrPV and TrV are shed in the insect's feces and represent a source of infection [22, 23]. Once the feces are deposited on the field or in insect nests, they are exposed to hot and dry ambient conditions (figure S1, supplemental information SI (stacks.iop.org/JPhysCM/30/104001/mmedia)). Although all these observations suggest that virus particles are able of surviving dry environments, little is known about how the lack of water affects the capsid structure.

Atomic force microscopy (AFM) provides both high-resolution images and physical properties of virus particles in liquid milieu [24]. AFM topographies allow for measuring the integrity of individual virus particles adsorbed on a solid substrate. Specifically, the particle dimensions (height and width) are an important indicator of the virus' structural integrity. This way, any structural change of the particle would result in a decrease of height [25], which may reflect either a structural collapse or just deformation. For instance, virus particles adsorbed on a surface in solution normally present a similar height to the nominal diameter obtained from the structural models [26–31]. Although it might depend on the virus–surface interplay [32], the interaction between virus capsids and the surface is usually not strong enough to induce important alterations on their structure in liquid. However, the subsequent desiccation by removing the water from the surface modifies the virus structure, which renders a height considerably lower than the hydrated values [33]. This structural alteration of the virus is due to several mechanisms. First, the lack of water contributes to the destabilization of the native folding and association of capsid subunits [34]. Second, capillary forces occurring during the final desiccation steps pulls the virus structure toward the substrate [33]. Third, dehydration changes the genome folding and its interaction with the viral capsid. The magnitude of this structural change deeply depends on the presence of viral genome inside the viral cavity. For instance, phage phi29 exhibited disrupted structures keeping about 6% and 36% of the hydrated height for empty and dsDNA full particles, respectively. Furthermore, full virus particles expel their genome out of the capsid shell [33]. The capillary forces of the water menisci formed in the virus during the last stages of dehydration triggered these structural changes. Specifically, freeze drying of virus structures avoid menisci formation and reduce virus collapse during dehydration process [30]. These forces strongly depend on the existence of nanometric channels and pores at the virus shell that regulate the way that the water escapes from the virus [35].

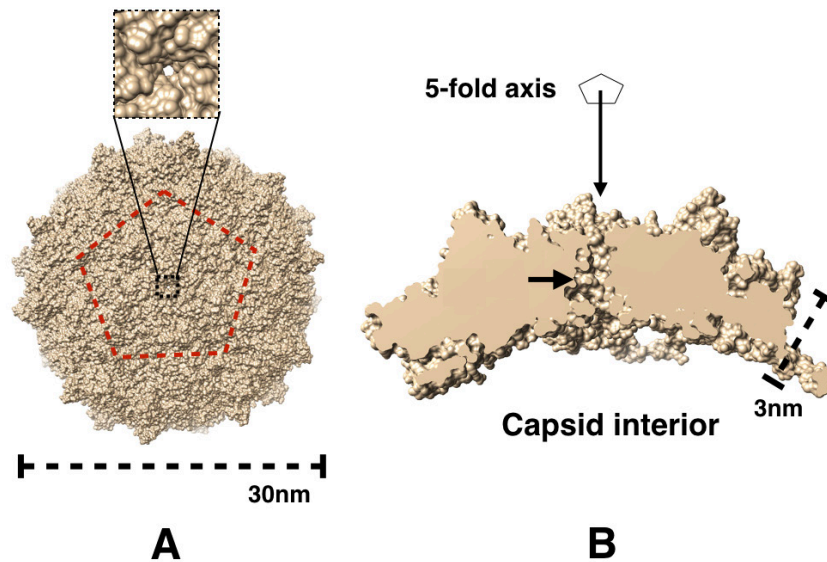


Figure 1. (A) TrV structure. TrV capsid has icosahedral symmetry of about 30 nm in diameter, and is built of 60 copies of each of the structural proteins VP1–VP3 (PDB code 3NAP). A fourth small protein, VP4, is disordered and buried at the capsid interior in contact with the RNA. The dashed red line approximately contours a penton made of $5 \times$ VP1-3. The close-up view shows the entrance of the cavity located at the five-fold symmetry axis. (B) Lateral view of a slab showing the penton with the cavity that traverses the capsid along the five-fold axis (for the sake of clarity, one protomer, i.e. three proteins, were removed). The surface represented corresponds to the solvent-accessible area. The short arrow indicates the approximate position of the crystallographic electron density attributed to a divalent ion [13].

The atomic structures of both CrPV [12] and TrV have been solved. As expected from the likeness of their amino acid sequence, the folding and overall shape are very similar [13]. The TrV capsid is built of 180 proteins called VP1-4, and has a diameter of about 30 nm (figure 1(A)). One striking point observed in both TrV and CrPV crystallographic structures is a bump of electron density that blocks the cavity that traverses the capsid along the five-fold symmetry axis (figure 1(B)). This sand clock-like cavity is formed by the arrangement of symmetry-related amino acid side chains, measuring ~ 0.5 nm in diameter at its narrowest region.

In this work, we analyze the ability of TrV particles to resist dehydration by monitoring the height of their structures before and after desiccation. In particular, we investigate the influence of ssRNA on TrV particles' stability, as well as whether the genome remains within the capsid after desiccation. Concerning the TrV shell structure, we studied how the modulation of the hydrophobic character of the aforementioned cavities at the five-fold symmetry axis results in a structural modification of the capsid by analyzing its height after desiccation.

Results

Virus purification from both experimentally infected insect corpses and dry insect feces allowed us to obtain samples of mature TrV virus (mTrV) and empty TrV capsids (Ecap). These two particles could be easily separated by using a sucrose gradient centrifugation, and characterized by UV absorption spectroscopy and TEM [17]. The average yield per gram of dry feces of mTrV and Ecap was about 0.25 mg and 1.2 mg, respectively. When the starting material was the abdomen of dry insect corpses, the Ecap content with respect to mTrV

was higher than that resulting from dry feces (Materials and Methods, MM). The diameter of both mTrV and Ecap particles as measured with dynamic light scattering (DLS) and as estimated from TEM experiments was about 30 nm. This value is coincident with the size determined from the crystallographic structure [13] and from cryo-TEM reconstructions [18] (figure 1(A)). After being treated with chelating agent, the samples of both particles did not experience any structural change, neither in height nor shape (SI figure S2). Moreover, we did not observe the disassembly by-products that could be indicative that removing ions from the structure affected particle stability.

Figure 2(A) shows a typical AFM topography of a single TrV particle obtained in the liquid condition. As usual [26, 27] the topographical profile, indicated by the blue arrows and depicted in figure 2(G) (blue), indicates that the particle height (~ 30 nm) is very close to the nominal diameter provided by the crystallographic atomic model (PDB code 3NAP; figure 1(A)). This fact indicates that in our case the virus-surface interaction hardly affects the virus' particle structure.

The surface is subsequently air dried by blowing with N_2 gas for a few seconds. Desiccation of TrV virions results in rounded structures (figure 2(B)), showing the suppression of capsomeric resolution. The topographical profile (red arrows in figure 2(B)) demonstrates that the particle height decreases to ~ 23 nm (red, figure 2(G)). AFM images do not show any indication of genome on the surface after desiccation (SI figure S4). In order to investigate the influence of the pore's character on the integrity of the TrV, we performed similar experiments with viral capsids treated with a chelating agent [36–39], as explained in MM. This treatment most likely removes the cation from each hydrophobic gate located at the five-fold symmetry axis [40]. The topographical profiles of the particles imaged in liquid milieu (figure 2(C)) show

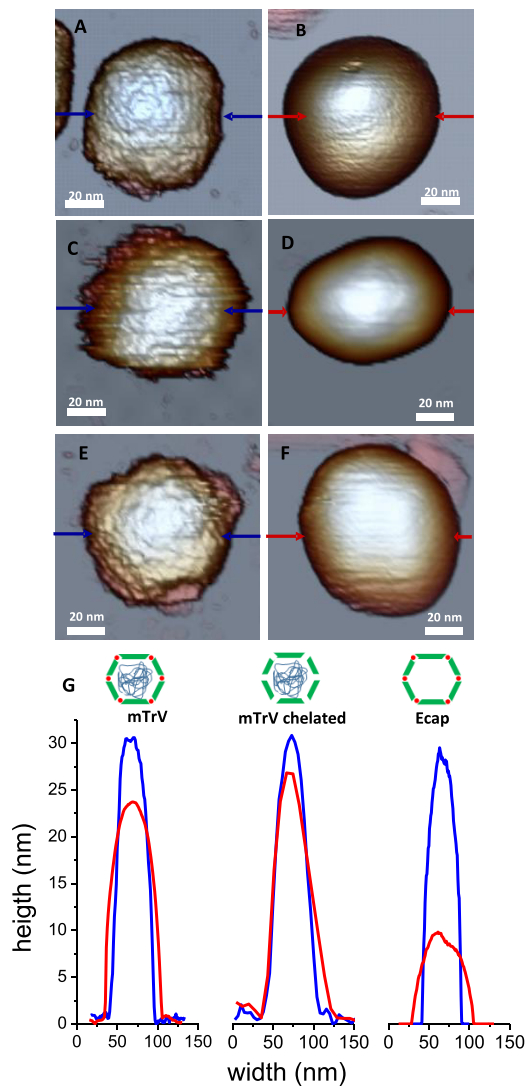


Figure 2. AFM of TrV capsids. Image (A) shows a topography of a TrV virion in liquid milieu, fully hydrated. Image (B) portrays the topography of a virion after desiccation. This topography shows a hole that might correspond to either a missing protein or a missing capsomer. Image (C) exhibits a chelated TrV virion, and (D) an example of a dehydrated one. Images (E) and (F) represent hydrated and dehydrated examples of Ecap structures, respectively. (G) displays the topographical profiles obtained in images (A)–(F) for comparison of the integrity of particles before (blue) and after (red) dehydration.

once more a height similar to the nominal diameter (blue, figure 2(G)). After desiccation, the chelated particle results again in a featureless structure (figure 2(D)). However, its profile (red, figure 2(G)) reaches higher values (~27 nm) than particles with ions still located at the hydrophobic gates. For the sake of comparison, figures 2(E) and (F) show examples of empty Ecap under liquid and dried conditions, whose profiles (figure 2(G)) show a dramatic collapse of the structure in air conditions.

Figure 3 displays the statistics of TrV particle height before and after drying. The diameter after desiccation of non-chelated and chelated particles is 25.3 nm and 27.2 nm,

respectively. An ANOVA test between the two virus populations demonstrates a confidence $p < 0.05$ that accounts for a significant difference (asterisks in figure 3). These results suggest that the ion observed in the five-fold symmetry axis plays an active role in the hydration of the virions. Besides height, AFM also provides the lateral dimensions of single TrV viruses (SI figure S5). These data indicate a certain propensity to flattening of virus particles upon desiccation, albeit with a high dispersion. Although this flattening is related to the deformation of particles during desiccation, we cannot neglect the inherent sample dilation originated by the lateral dimension of the tip [41].

Discussion

Viruses are biomolecular assemblies that necessitate liquid milieu to replicate. As any other biomolecule, dehydration might affect their structure and functionality. The achievement of resistance against desiccation would require the viral capsids to keep their structural integrity as much as possible. Although other biological structures such as spores can withstand long periods under dry condition [42], being spherical viruses hollow structures containing moieties, little is known about how viruses retain their solvent content. In a previous work, we observed in two geometrically different icosahedral non-enveloped dsDNA viruses that desiccation causes genome ejection from the capsid [33], leaving faulty structures for infection. Drying studies run by another group on HAV and PV, two virus capsids belonging to the *Enterovirus* family, showed that when dried in environmental fomites, HAV is more resistant to inactivation than PV [43].

Role of structural ions in icosahedral viruses

Although the exact identity of ions found in different viruses has not been extensively determined, we do know that there are metal binding sites on the five-fold axis of many virus capsids [10]. The main role these ions play in the capsid is *structural*, in the sense that they confer to the overall structure certain properties that are not associated with large changes in the protein fold. This can be illustrated by the fact that in both HRV14 and HRV16 the metal ions may play a role in viral disassembly, but no conformational changes are observed in the viral structures when the ions are removed [10]. In the case of TrV, it is also observed that the five-fold cavity of the virions capsid that contains the cations changes subtly changes in response to the capsid without cations [19]. It is obvious that in order for a cation to be part of a protein atomic structure, very stringent electronic conditions have to be fulfilled. However, if the protein structure is almost the same for both cavities (with and without ions), where does the structural difference reside? In light of our previous results modeling the solvation of the TrV capsid [40], the presence of the cation at the five-fold symmetry axis could determine the hydration of the cavity.

The role of ssRNA

Previous experiments [33] demonstrated that the existence of genome within the viral cavity prevents the collapse of dsDNA viral capsids. TrV capsids demonstrate a similar behavior, and empty Ecap particles collapse dramatically after desiccation. In this case, we find that empty particles reduce their height to 9 nm, about 30% of the hydrated value (figure 3). However, mTrV capsids decrease their height to 84% of the hydrated value. This fact reveals that ssRNA in TrV, as dsDNA in other viruses, is an important contributor to keeping the virus structure under desiccation. In fact, the height of collapsed Ecap structures is very close to the thickness of two TrV capsid walls (~6 nm, figure 1(B)). However, the most striking feature we found is that, in contrast with other viruses such as phi29 bacteriophage or the Minute Virus of Mice [33], TrV capsids keep their genome inside after desiccation. This property seems quite adequate for TrV, which withstands stringent drying during long periods along its horizontal transmission, whereas feces dry in a few hours. If RNA leaves the capsid during dehydration, it seems very unlikely for it to be packed back in again without expressing new protein shells: this only happens in the cell environment. Consequently, for viruses transmitted through the fecal–oral route, retaining the genome inside the capsid during ambient exposure might constitute a necessary condition to complete the infection cycle.

Altogether, our experiments reveal that in TrV, and most likely in other similar viruses containing ions at the five-fold axis, the capsid's resistance to dehydration stress seems to be favored by the packed genome but disfavored by these structural ions. Nevertheless, one of the necessary features that permit the horizontal transmission of the virus in dry natural environments may be that the TrV capsid maintains its genome under stringent dehydration conditions. This feature could affect the recovery of TrV structural and infectious characteristics under proper hydration conditions, either in feces or the insect digestive tract. Therefore, a challenging experiment consists of characterizing the capsid structures with AFM after rehydrating the dried viruses adsorbed on the surface. Figure S6 (SI) presents an example of such experiment, showing a very inhomogeneous sample of unidentified specimens where it is difficult to separate virus particles from debris. We think that our experiment is probably not mimicking the natural rehydration conditions, and more effort should be invested in addressing this issue. We speculate that TrV being capable of keeping RNA inside under dehydrated ambient conditions is the result of evolutionary adaptation of this and other similar viruses to favor horizontal transmission.

Structural ions favor draining the internal solvent

Since the cavity along the five-fold icosahedral axis has a small neck, this structural feature can be considered as a barrier for the solvent to freely permeate the capsid shell. In fact, simulation studies of narrow cavities in membrane protein structures coin the concept of the 'hydrophobic gate' [44–46].

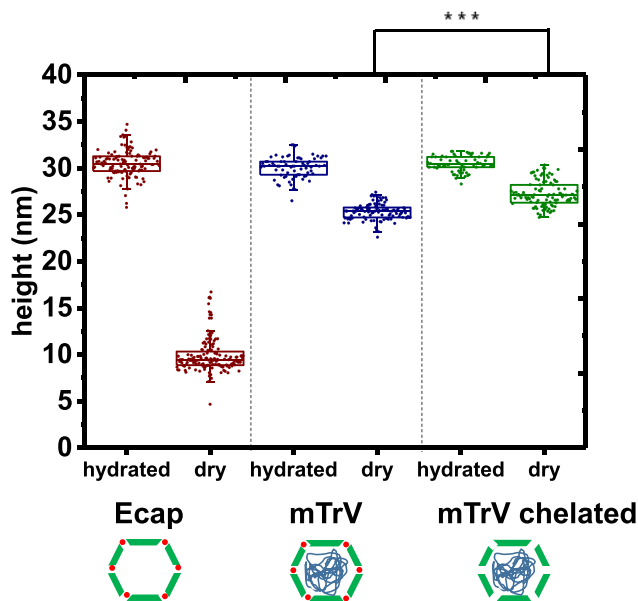


Figure 3. Changes of TrV capsids height after desiccation. This box plot contains the statistical analysis of 145 empty particles, 100 virions, and 100 chelated particles in red, blue, and green colors, respectively.

Meanwhile, calculations show that the water density within cylindrical cavities with a diameter below 0.7 nm can be described as in a liquid–vapor transition [47]. This behavior depends on the pore diameter and hydrophobic/hydrophilic character of the amino acid lining the cavity. More recent experimental studies done in non-biological nanopores gave direct evidence of hydrophobic gating modulated by applying a voltage across the pore [48]. Our previous simulation of the TrV capsid [40] found that the hydrophobic barrier is removed if the divalent cation is placed in a point in the cavity that crystallographic studies assign to a coordinated ion [13]. When the ion is present, the cavity is fully hydrated and water molecules enter the hydrophobic neck, forming a line [40]. Due to the key role water molecules play in biological systems, the conduction of solvent and ions through proteins attracts the interest of both theoretical and experimental studies. In particular, the aquaporin family of water pores provides a remarkable example of water conduction through long (ca. 2 nm) and narrow (about 0.3 nm) means of traversing a protein body [45, 49, 50]. Since virus wall is the border of the virion with the external environment, its structure and porosity determine the release of water during desiccation [35]. In this respect, the hydrophobic character of the 12 transversal channels at the pentons of TrV capsid seems to influence the structure of virus particles after desiccation. Chelated particles, where the divalent ion has been removed from the channels, keep about 90% of the hydrated height (figure 3). However, the presence of divalent cations in TrV particles preserves about the 84% of the hydrated height (figure 3). When the hydrophobic character of the channels is active (chelated particles), virus capsids exhibit a larger height. We interpret that the hydrophilic character of these channels favors the water to escape from the virus cavity, removing water from the RNA.

However, the hydrophobic channels (without ions) do not promote the water to leave, and the RNA remains hydrated. We suggest that the hydrated nucleic acids prevent virus deformation more efficiently than a dehydrated genome because the presence of water stabilizes the RNA's folding and structure [51–54]. It is important to remark that both chelated and non-chelated particles do not result in collapse, but deformed structures after dehydration. However, according to figure S5, mTrV particles show higher deformation because their full width at half maximum (FWHM) is larger than that of the chelated mTrV. The ions' role of facilitating water escape contrasts with the intuitive thinking that the presence of ions should block the viral cavity. The presence or absence of ions might be useful in a natural environment in two ways. It is important to shuttle the water in and out to, on one hand, maximize virus stability during dry conditions and, on the other hand, allow hydration when needed for activating the virus for infection again.

In addition to this regulatory function in regulating capsid hydration, based on molecular dynamic and quantum calculations we postulate that the cavities at the five-fold axis could function as ion channels. This is because a positive cation like Ca or Mg trapped in the hydrophobic and narrowest part of cavity (ca. 5 Å in diameter) can attract water molecules to enter the cavity. This hydration could form a 'water wire' and span about 2.0 nm long. Under this condition, our calculations indicate that the water wire connect the outer and inner solvent bulk regions, thus allowing protons to exit from the capsid interior. This arrangement located at the five-fold cavity and formed by the cation and water wire would function as a pH sensor [37].

Conclusion

Our work demonstrates that, compared with other viruses, the TrV capsid better supports dehydration conditions by keeping the genome inside. In addition, we also showed how the presence/absence of structural ions at the five-fold axis of TrV virions modulate their stability against dehydration. Our results suggest that the role of the cation is not only to hydrate the cavity, but also to favor the leakage of solvent from the capsid interior. Our work paves the way for understanding the structural factors affecting viruses when dehydration takes place.

Materials and methods

Rearing insects in insectary

A TrV-infected triatomine has been maintained at the Center for Studies and Parasitological Vectors since 2002, originating from field-collected insects infected with TrV. The insects are held at 28 ± 1 °C, $60\% \pm 5\%$ relative humidity, and a photoperiod of 12:12 h (light:dark). Since insects of this colony composed of about 300–400 individuals die due to the infection, the colony is maintained by the incorporation of 100 monthly healthy nymphs free of TrV. The triatomines are in 400 cm³ plastic containers covered with a nylon mesh, and are provided with vertical paper strips as resting places. The insects are fed every 15 d and prior to feeding the paper is removed in order to collect the dry fecal material.

TrV purification

Mature viral particles (containing viral RNA, mTrV) were obtained from dry feces collected in the rearing containers of an experimentally infected triatomine's insect colony. First, 100 ml of lysis buffer (10 mM NaCl, 1 mM MgCl₂, 200 mM citric acid, pH 6.0) was added per gr of dry material. PMSF was then added to achieve a final concentration of 1 mM. In order to disrupt clusters of feces, samples were first vortexed for 5 min, and then sonicated at 4 °C by several 20 s pulses. Samples were then centrifuged for 45 min, at 4 °C and 12 000 rpm (Optima L-90 K centrifuge, Beckman Coulter). Supernatant was further centrifuged 2.5 h, 40 000 rpm (Optima L-90 K centrifuge, Beckman Coulter). Pellets were then resuspended overnight at 4 °C in 2 ml NMT buffer (10 mM NaCl, 1 mM MgCl₂, 50 mM Tris-HCl, pH 7.4).

Empty viral particles were obtained from intestines of dead dried insects, and 15 ml of NMT buffer was added to each gr of material, containing 1 mM PMSF. Then, samples were vortexed for 5–10 min, then shook for 20–30 min. at 4 °C, and finally sonicated at 4 °C (10 s ON, 15 s OFF, 20 pulse in an MSE Soniprep 150 sonicator). Samples were then centrifuged for 30 min at 4 °C and 14 500 rpm (Optima L-90 K centrifuge, Beckman Coulter). The supernatant was further centrifuged for 3 h at 4 °C and 44 000 rpm (Optima L-90 K centrifuge, Beckman Coulter). Pellets containing viral particles were resuspended overnight at 4 °C in 1 ml NMT buffer.

In order to separate mature and empty viral particles from other materials, chromatography in sucrose gradient was performed. The resuspended material was loaded in a 5–30% sucrose gradient column and centrifuged for 3 h at 4 °C and $100\,000 \times g$. Fractions of 0.5–1 ml were collected and stored on ice. In order to check protein content, fractions were analyzed by SDS-PAGE in 12.5% acrylamide gels and developed with Coomassie staining. Collected fractions showing the highest protein content were pooled together. In order to remove the sucrose, the pooled samples from the sucrose gradient were dialyzed overnight at 4 °C against 2 l NMT buffer.

Protein concentration was then measured by absorbance at 280 nm (NanoDrop 2000, Thermo Scientific™).

Sample concentrations

Particle viral samples were concentrated to 0.2 mg ml⁻¹ (for chelating treatment) or to 1 mg ml⁻¹ (for AFM analysis) by dialysis, using a Millipore membrane filter of 30 kDa cut-off (Amicon® Ultra-4, Amicon) centrifuging at room temperature and $4500 \times g$; each centrifugation was no more than 3 min. In those cases where the final concentration was higher than required, samples were diluted with NMT buffer.

Chelation of mTrV structural ions

In order to extract from the TrV capsid all solvent-exposed ions, including the putative ion located at each pore of each symmetry axis, samples of purified mTrV were chelated with EDTA (ethylenediamine tetra-acetic acid). Then, 4 ml (0.2 mg ml⁻¹) of purified virus were dialyzed overnight at 4 °C against

2 l of NT buffer (50mM Tris-HCl, 10mM NaCl) containing 100mM EDTA. Control samples were dialyzed in the same conditions, but against 2 l of NT Buffer without EDTA. Then, in order to eliminate/dilute the EDTA from the solutions, samples were dialyzed (3–4h, 4 °C) once more against 2 l of NT buffer.

Dynamic light scattering measurement

The height of both TrV empty capsids and virion were measured using a Zetaheight Nano S (Malvern, UK) DLS, which employs a 5 mW He–Ne laser emitting at 633 nm and a photomultiplier oriented at 173° from the incident beam. The particles were dissolved in NMT buffer and in a concentration (protein) of about 0.2 mg ml⁻¹. Samples were placed into Uvette plastic cuvettes, and the particle diameter was averaged from 12 independent measurements automatically performed by the equipment. These measurements represent the hydrodynamic diameter as deduced from the Stokes equation.

TEM measurements

Images of TrV of empty particles, full virions, and full virions after chelating treatment were observed with TEM. Images were acquired using a Phillips EM208S TEM equipped with a Morada camera (nominal resolution of 0.34 nm). A sample stain was done using uranyl acetate (2%), and particle solutions for these studies were at a concentration of about 0.1 mg ml⁻¹ (protein). The samples were mounted on polarized (glow discharge method) carbon-coated copper grids.

AFM measurements and virus dehydration

For AFM imaging, virus samples were diluted in a solution of NT/NMT to obtain a final concentration of 0.02 mg ml⁻¹ (protein concentration). A drop of 30 µl of virus solution was deposited on freshly cleaved highly oriented pyrolytic graphite and incubated for 20 min at room temperature before washing with NT/NMT buffer. After incubation, the sample was immersed in 200 µl of the same buffer that was used before. The sample was therefore maintained in a hydrated, close to physiological state throughout the experiment. (SI figure S3). In the case of dehydration, samples were equally prepared, but the water meniscus was removed by blowing with N₂, and imaging was done in dynamic mode (SI figure S3).

The AFM (Nanotec Electrónica) was operated in jumping mode, and in liquid and amplitude modulation modes in air, using RC800PSA (Olympus) cantilevers with nominal spring constants of 0.05 and 0.39 N m⁻¹ respectively [55]. Cantilevers were routinely calibrated using Sader's method [56]. AFM imaging was performed at 70 pN to explore the viruses on the surface in liquid. In air, we used the non-contact dynamic mode [57].

Acknowledgments

TEM images were collected at the Servicio General de Microscopía Analítica y de Alta Resolución en

Biomedicina (SGIKER, UPV/EHU). PJP thanks FIS2014-59562-R, FIS2015-71108-REDT, Fundación BBVA and 'María de Maeztu' Program for Units of Excellence in R&D (MDM-2014-0377), and FIS2017-89549-R. DMAG thanks the Servicio de Microscopía Analítica y de Alta Resolución en Biomedicina of SGIker (UPV/EHU) for TEM measurements. GAM is a staff member of CONICET. This work was partially supported by a grant to DMAG from the Ministerio de Ciencia e Innovación (BFU2012-36241), and Gobierno Vasco (Elkartek KK-2017/00008), Spain. SMGD thanks the Fundación Biofísica Bizkaia, Spain, for traveling support to visit PJP's lab. GAM and DMAG acknowledge a grant from the CYTED (216RT0506). GAM is recipient of grants from the Agencia Nacional de Promoción Científica y Técnica (PICT N° 2014-1536 and 2015-0665), Argentina.

ORCID iDs

Diego M A Guérin  <https://orcid.org/0000-0001-8504-9636>
Pedro J de Pablo  <https://orcid.org/0000-0003-2386-3186>

References

- [1] Laidler J R, Shugart J A, Cady S L, Bahjat K S and Stedman K M 2013 Reversible inactivation and desiccation tolerance of silicified viruses *J. Virol.* **87** 13927–9
- [2] Roden R B, Lowy D R and Schiller J T 1997 Papillomavirus is resistant to desiccation, *J. Infect. Dis.* **176** 1076–9
- [3] Boone S A and Gerba C P 2007 Significance of fomites in the spread of respiratory and enteric viral disease *Appl. Environ. Microbiol.* **73** 1687–96
- [4] Fogarty R, Halpin K, Hyatt A D, Daszak P and Mungall B A 2008 Henipavirus susceptibility to environmental variables *Virus Res.* **132** 140–4
- [5] Ding D C, Chang Y C, Liu H W and Chu T Y 2011 Long-term persistence of human papillomavirus in environments *Gynecol. Oncol.* **121** 148–51
- [6] Palich R, Ireng L M, Barte de Sainte Fare E, Augier A, Malvy D and Gala J-L 2017 Ebola virus RNA detection on fomites in close proximity to confirmed Ebola patients; N'Zerekore, Guinea, 2015 *PLoS One* **12** e0177350
- [7] Hogle J M, Chow M and Filman D J 1985 Three-dimensional structure of poliovirus at 2.9 Å resolution *Science* **229** 1358–65
- [8] Wang X *et al* 2015 Hepatitis A virus and the origins of picornaviruses *Nature* **517** 85–8
- [9] Rossmann M G *et al* 1985 Structure of a human common cold virus and functional relationship to other picornaviruses *Nature* **317** 145–53
- [10] Zhao R, Hadfield A T, Kremer M J and Rossmann M G 1997 Cations in human rhinoviruses *Virology* **227** 13–23
- [11] Hadfield A T, Lee W, Zhao R, Oliveira M A, Minor I, Rueckert R R and Rossmann M G 1997 The refined structure of human rhinovirus 16 at 2.15 Å resolution: implications for the viral life cycle *Structure* **5** 427–41
- [12] Tate J, Liljas L, Scotti P, Christian P, Lin T and Johnson J E 1999 The crystal structure of cricket paralysis virus: the first view of a new virus family *Nat. Struct. Biol.* **6** 765–74
- [13] Squires G, Pous J, Agirre J, Rozas-Dennis G S, Costabel M D, Marti G A, Navaza J, Bressanelli S, Guerin D M and Rey F A 2013 Structure of the *Triatoma* virus capsid *Acta Crystallogr. D* **69** 1026–37
- [14] Unge T, Montelius I, Liljas L and Ofverstedt L G 1986 The EDTA-treated expanded satellite tobacco necrosis

- virus: biochemical properties and crystallization *Virology* **152** 207–18
- [15] Montelius I, Liljas L and Unge T 1990 Sequential removal of Ca^{2+} from satellite tobacco necrosis virus. Crystal structure of two EDTA-treated forms *J. Mol. Biol.* **212** 331–43
- [16] Rozas Dennis G S, La Torre J L, Muscio O A and Guérin D M A 2000 Direct methods for detecting picorna-like virus from dead and alive Triatomine insects *Memórias do Instituto Oswaldo Cruz* **95** 323
- [17] Agirre J, Aloria K, Arizmendi J M, Iloro I, Elortza F, Sánchez-Eugenia R, Marti G A, Neumann E, Rey F A and Guérin D M A 2011 Capsid protein identification and analysis of mature *Triatoma virus* (TrV) virions and naturally occurring empty particles *Virology* **409** 91–101
- [18] Agirre J, Goret G, LeGoff M, Sanchez-Eugenia R, Marti G A, Navaza J, Guerin D M and Neumann E 2013 Cryo-electron microscopy reconstructions of *Triatoma virus* particles: a clue to unravel genome delivery and capsid disassembly *J. Gen. Virol.* **94** 1058–68
- [19] Sanchez-Eugenia R, Durana A, Lopez-Marijuan I, Marti G A and Guerin D M 2016 X-ray structure of *Triatoma virus* empty capsid: insights into the mechanism of uncoating and RNA release in dicistroviruses *J. Gen. Virol.* **97** 2769–79
- [20] Bonning B C and Miller W A 2010 Dicistroviruses *Annu. Rev. Entomol.* **55** 129–50
- [21] Marti G A, Gonzalez E T, Garcia J J, Viguera A R, Guerin D M and Echeverria M G 2008 AC-ELISA and RT-PCR assays for the diagnosis of *Triatoma virus* (TrV) in triatomines (*Hemiptera: Reduviidae*) species *Arch. Virol.* **153** 1427–32
- [22] Manousis T and Moore N F 1987 Cricket paralysis virus, a potential control agent for the olive fruit fly, *Dacus oleae* Gmel *Appl. Environ. Microbiol.* **53** 142
- [23] Muscio O, Bonder M A, La Torre J L and Scodeller E A 2000 Horizontal transmission of *Triatoma virus* through the fecal-oral route in *Triatoma infestans* (*Hemiptera: Triatomidae*) *J. Med. Entomol.* **37** 271–5
- [24] Moreno-Madrid F, Martín-González N, Llauro A, Ortega-Esteban A, Hernando-Pérez M, Douglas T, Schaap I A and de Pablo P J 2017 Atomic force microscopy of virus shells *Biochem. Soc. Trans.* **45** 499–511
- [25] Ortega-Esteban A, Perez-Berna A J, Menendez-Conejero R, Flint S J, Martin C S and de Pablo P J 2013 Monitoring dynamics of human adenovirus disassembly induced by mechanical fatigue *Sci. Rep.* **3** 1434
- [26] Llauro A, Schwarz B, Koliyatt R, de Pablo P J and Douglas T 2016 Tuning viral capsid nanoparticle stability with symmetrical morphogenesis *ACS Nano* **10** 8465–73
- [27] Llauro A, Luque D, Edwards E, Trus B L, Avera J, Reguera D, Douglas T, Pablo P J and Caston J R 2016 Cargo-shell and cargo-cargo couplings govern the mechanics of artificially loaded virus-derived cages *Nanoscale* **8** 9328–36
- [28] Ortega-Esteban A, Condezo G N, Perez-Berna A J, Chillón M, Flint S J, Reguera D, San Martín C and de Pablo P J 2015 Mechanics of viral chromatin reveals the pressurization of human adenovirus *ACS Nano* **9** 10826–33
- [29] Llauro A, Coppari E, Imperatori F, Bizzarri A R, Caston J R, Santi L, Cannistraro S and de Pablo P J 2015 Calcium ions modulate the mechanics of tomato bushy stunt virus *Biophys. J.* **109** 390–7
- [30] Hernando-Pérez M, Lambert S, Nakatani-Webster E, Catalano C E and de Pablo P J 2014 Cementing proteins provide extra mechanical stabilization to viral cages *Nat. Commun.* **5** 4520
- [31] Snijder J, Utrecht C, Rose R J, Sanchez-Eugenia R, Marti G A, Agirre J, Guerin D M, Wuite G J, Heck A J and Roos W H 2013 Probing the biophysical interplay between a viral genome and its capsid *Nat. Chem.* **5** 502–9
- [32] Zeng C, Hernando-Pérez M, Dragnea B, Ma X, van der Schoot P and Zandi R 2017 Contact mechanics of a small icosahedral virus *Phys. Rev. Lett.* **119** 038102
- [33] Carrasco C, Douas M, Miranda R, Castellanos M, Serena P A, Carrascosa J L, Mateu M G, Marques M I and de Pablo P J 2009 The capillarity of nanometric water menisci confined inside closed-geometry viral cages *Proc. Natl Acad. Sci. USA* **106** 5475–80
- [34] Zlotnick A 2003 Are weak protein-protein interactions the general rule in capsid assembly? *Virology* **315** 269–74
- [35] Serena P A, Douas M, Marques M I, Carrasco C, de Pablo P J, Miranda R, Carrascosa J L, Castellanos M and Mateu M G 2009 MC simulations of water meniscus in nanocontainers: explaining the collapse of viral particles due to capillary forces *Phys. Status Solidi c* **6** 2128–32
- [36] Li P P, Nakanishi A, Tran M A, Ishizu K, Kawano M, Phillips M, Handa H, Liddington R C and Kasamatsu H 2003 Importance of Vp1 calcium-binding residues in assembly, cell entry, and nuclear entry of simian virus 40 *J. Virol.* **77** 7527–38
- [37] Ruiz M C, Cohen J and Michelangeli F 2000 Role of Ca^{2+} in the replication and pathogenesis of rotavirus and other viral infections *Cell Calcium* **28** 137–49
- [38] Lee C C, Ko T P, Chou C C, Yoshimura M, Doong S R, Wang M Y and Wang A H 2006 Crystal structure of infectious bursal disease virus VP2 subviral particle at 2.6 Å resolution: implications in virion assembly and immunogenicity *J. Struct. Biol.* **155** 74–86
- [39] Wilts B D, Schaap I A and Schmidt C F 2015 Swelling and softening of the cowpea chlorotic mottle virus in response to pH shifts *Biophys. J.* **108** 2541–9
- [40] Viso J, Belli P, Machado M, González H, Pantano S, Zamarreño M J F, Branda M M, Guérin D M A and Costabel M D 2017 Multiscale Modelization in a Small Virus: Mechanism of proton channeling and its role in triggering the capsid disassembly, in preparation
- [41] Villarrubia J S 1997 Algorithms for scanned probe microscope image simulation, surface reconstruction, and tip estimation *J. Res. Natl Inst. Stand. Technol.* **102** 425–54
- [42] Van Der Hofstadt M, Fabregas R, Millan-Solsona R, Juarez A, Fumagalli L and Gomila G 2016 Internal hydration properties of single bacterial endospores probed by electrostatic force microscopy *ACS Nano* **10** 11327–36
- [43] Abad F X, Pinto R M and Bosch A 1994 Survival of enteric viruses on environmental fomites *Appl. Environ. Microbiol.* **60** 3704
- [44] Allen R, Melchionna S and Hansen J P 2002 Intermittent permeation of cylindrical nanopores by water *Phys. Rev. Lett.* **89** 175502
- [45] Beckstein O and Sansom M S 2003 Liquid-vapor oscillations of water in hydrophobic nanopores *Proc. Natl Acad. Sci. USA* **100** 7063–8
- [46] Beckstein O and Sansom M S 2004 The influence of geometry, surface character, and flexibility on the permeation of ions and water through biological pores *Phys. Biol.* **1** 42–52
- [47] Beckstein O, Biggin P C, Bond P, Bright J N, Domene C, Grottesi A, Holyoake J and Sansom M S 2003 Ion channel gating: insights via molecular simulations *FEBS Lett.* **555** 85–90
- [48] Powell M R, Cleary L, Davenport M, Shea K J and Siwy Z S 2011 Electric-field-induced wetting and dewetting in single hydrophobic nanopores *Nat. Nanotechnol.* **6** 798–802
- [49] Kung C, Martinac B and Sukharev S 2010 Mechanosensitive channels in microbes *Annu. Rev. Microbiol.* **64** 313–29
- [50] Guo W, Tian Y and Jiang L 2013 Asymmetric ion transport through ion-channel-mimetic solid-state nanopores *Acc. Chem. Res.* **46** 2834–46
- [51] Moreno-Herrero F, Colchero J and Baro A M 2003 DNA height in scanning force microscopy *Ultramicroscopy* **96** 167–74

- [52] Moreno-Herrero F, Colchero J, Gomez-Herrero J and Baro A M 2004 Atomic force microscopy contact, tapping, and jumping modes for imaging biological samples in liquids *Phys. Rev. E* **69** 031915
- [53] Jana B, Pal S, Maiti P K, Lin S-T, Hynes J T and Bagchi B 2006 Entropy of water in the hydration layer of major and minor grooves of DNA *J. Phys. Chem. B* **110** 19611–8
- [54] Khesbak H, Savchuk O, Tsushima S and Fahmy K 2011 The role of water H-bond imbalances in B-DNA substate transitions and peptide recognition revealed by time-resolved FTIR spectroscopy *J. Am. Chem. Soc.* **133** 5834–42
- [55] Ortega-Esteban A, Horcas I, Hernando-Perez M, Ares P, Perez-Berna A J, San Martin C, Carrascosa J L, de Pablo P J and Gomez-Herrero J 2012 Minimizing tip-sample forces in jumping mode atomic force microscopy in liquid *Ultramicroscopy* **114** 56–61
- [56] Sader J E, Chon J W M and Mulvaney P 1999 Calibration of rectangular atomic force microscope cantilevers *Rev. Sci. Instrum.* **70** 3967–9
- [57] de Pablo P J, Colchero J, Luna M, Gomez-Herrero J and Baro A M 2000 Tip-sample interaction in tapping-mode scanning force microscopy *Phys. Rev. B* **61** 14179–83